Hydrogen-Bonding Alterations of the Protonated Schiff Base and Water Molecule in the Chloride Pump of *Natronobacterium pharaonis*†

Mikihiro Shibata,‡ Norikazu Muneda,‡ Takanori Sasaki,§ Kazumi Shimono,|| Naoki Kamo,|| Makoto Demura,§ and Hideki Kandori*,‡

Department of Materials Science and Engineering, Nagoya Institute of Technology, Showa-ku, Nagoya, 466-8555, Japan, Department of Biological Sciences, Graduate School of Science, Hokkaido University, Sapporo 060-0812, Japan, and Laboratory of Biophysical Chemistry, Graduate School of Pharmaceutical Sciences, Hokkaido University, Sapporo 060-0812, Japan

Received April 19, 2005; Revised Manuscript Received July 11, 2005

ABSTRACT: Halorhodopsin is a light-driven chloride ion pump. Chloride ion is bound in the Schiff base region of the retinal chromophore, and unidirectional chloride transport is probably enforced by the specific hydrogen-bonding interaction with the protonated Schiff base and internal water molecules. In this article, we study hydrogen-bonding alterations of the Schiff base and water molecules in halorhodopsin of *Natronobacterium pharaonis* (*p*HR) by assigning their N−D and O−D stretching vibrations in D_2O, respectively. Highly accurate low-temperature Fourier transform infrared spectroscopy revealed that hydrogen bonds of the Schiff base and water molecules are weak in the unphotolyzed state, whereas they are strengthened upon retinal photoisomerization. Halide dependence of the stretching vibrations enabled us to conclude that the Schiff base forms a direct hydrogen bond with Cl^- only in the K intermediate. Hydrogen bond of the Schiff base is further strengthened in the L_1 intermediate, whereas the halide dependence revealed that the acceptor is not Cl^-, but presumably a water molecule. Thus, it is concluded that the hydrogen-bonding interaction between the Schiff base and Cl^- is not a driving force of the motion of Cl^-. Rather, the removal of its hydrogen bonds with the Schiff base and water(s) makes the environment around Cl^- less polar in the L_1 intermediate, which presumably drives the motion of Cl^- from its binding site to the cytoplasmic domain.

Photosynthesis in some archaea involves two rhodopsins, which do not utilize electron transfer reactions in the process. Bacteriorhodopsin (BR)[1] and halorhodopsin (HR) in *Halobacterium salinarum* function as light-driven proton and chloride pumps, respectively (*1*−*4*). The chromophore of these proteins is all-trans retinal that binds to a lysine residue through a Schiff base linkage, and the all-trans to 13-cis photoisomerization triggers the pumping process. Extensive studies on BR have suggested the mechanism for unidirectional translocation of protons (*1*, *2*). In contrast, the molecular mechanism of the chloride pump in *salinarum* HR (*s*HR) and a homologous HR from *Natronobacterium pharaonis* (*p*HR) is less understood.

In 2000, Kolbe et al. determined the crystal structure of *s*HR, which provided a structural picture of the chloride pump (*5*). Figure 1a shows the Schiff base region of *s*HR, which contains a quadrupole with positive charges located at the protonated Schiff base and at Arg108, and counterbalancing negative charges located at the chloride ion and Asp238 (*5*). The quadrupole inside the protein is stabilized by three water molecules (water22, -24, and -50). Similar structure is also preserved in BR, where the chloride ion is replaced by aspartate (Asp85) that corresponds to Thr111 in *s*HR. In BR, a water molecule is likely to bridge the Schiff base and Asp85, because the distances ($N-O_{water}$, 2.9 Å; $O_{water}-O_{Asp85}$, 2.6 Å) and geometry of these atoms ($N-O_{water}-O_{Asp85}$ angle, 105.5°) are ideal for strong hydrogen bonds (*6*). In contrast, Figure 1b suggests a different role for the "bridge" water (water22) in *s*HR, because the $N-O_{water}$ and $O_{water}-Cl^-$ distances are 3.3 and 3.1 Å, respectively, and the $N-O_{water}-Cl^-$ angle is 70.9°. The role of these water molecules in the chloride ion pump is intriguing.

It is believed that the interaction between the protonated Schiff base and Cl^- plays a crucial role in the vectorial transport of chloride ion. Therefore, it is essential to experimentally monitor the hydrogen-bonding strength of the Schiff base during the photocycle of HR. For this purpose, differences in frequency between C═NH and C═ND stretching vibrations were measured, the strong hydrogen bonds yielding larger differences (*7*, *8*). On this basis, earlier resonance Raman spectroscopy of *s*HR revealed that the hydrogen bond of the Schiff base is weaker in *s*HR than in BR (*9*), but becomes much stronger in the L intermediate (*10*). From the halide-dependent C═N stretching frequencies

† This work was supported by grants from Japanese Ministry of Education, Culture, Sports, Science, and Technology to H.K. (15076202).

* To whom correspondence should be addressed. Phone and fax: 81-52-735-5207. E-mail: kandori@nitech.ac.jp.

‡ Nagoya Institute of Technology.

§ Graduate School of Science, Hokkaido University.

|| Graduate School of Pharmaceutical Sciences, Hokkaido University.

[1] Abbreviations: BR, bacteriorhodopsin; *p*HR, *pharaonis* halorhodopsin; *s*HR, *salinarum* halorhodopsin; FTIR, Fourier transform infrared; pHR_K, K intermediate of *p*HR; pHR_{L1}, L_1 intermediate of *p*HR; pHR_{L2}, L_2 intermediate of *p*HR.

10.1021/bi050726d CCC: $30.25
Published on Web 08/23/2005

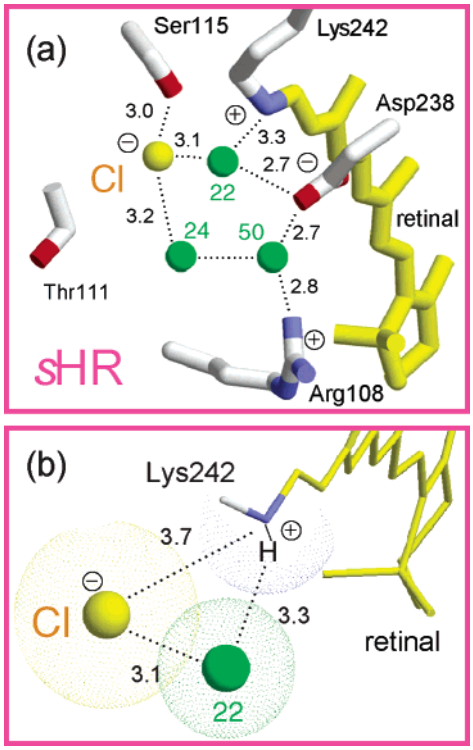

FIGURE 1: (a) Structure of the Schiff base region in *s*HR (PDB entry 1E12 (*5*)). The membrane normal is approximately in the vertical direction of this figure, and upper and lower regions correspond to the cytoplasmic and extracellular sides, respectively. Chloride ions are translocated upward in the figure. Green spheres represent water molecules in the Schiff base region. Dotted lines represent putative hydrogen bonds, whose distances are shown in Å. (b) The same structure viewed from a different angle. Van der Waals radii of the chloride ion, water22, and the nitrogen atom of the Schiff base are also shown.

in the L intermediate of *p*HR, Gerscher et al. suggested that the Schiff base directly interacts with Cl^- in the L intermediate (*11*). In contrast, earlier FTIR study observed similarly halide-dependent C=N stretches for *s*HR and the L intermediate, and proposed that the Schiff base forms a direct hydrogen bond with Cl^- both in *s*HR and in the L intermediate (*12*). Thus, a clear picture has never been established for the hydrogen-bonding interaction of the Schiff base and Cl^-. One reason could be that the C=N stretch is a skeletal vibration of the retinal chromophore, and even when the C=NH and C=ND frequency difference explains the hydrogen-bonding strength of the Schiff base well, halide dependence on the C=N stretch does not necessarily reflect hydrogen-bonding interaction of the Schiff base with halides. In fact, the reported difference in frequency among three halides (Cl^-, Br^-, and I^-) was within 0.4 and 2.6 cm^{-1} for *p*HR and the L intermediate, respectively (*11*), and within 3.1 and 3.7 cm^{-1} for *s*HR and the L intermediate, respectively (*12*).

The N−H stretching mode is the direct probe of the hydrogen-bonding strength of the Schiff base. In fact, Lussier et al. reported that the N−H stretching frequencies of the all-trans retinal protonated Schiff base in $CDCl_3$ are located at 2600, 2735, and 2957 cm^{-1} in the presence of Cl^-, Br^-, and I^-, respectively (*13*). In solution, halide ion is located at the most stable position relative to the Schiff base, where the Schiff base N−H group presumably forms a direct hydrogen bond with halide ion. Thus, we can state that if the Schiff base forms a hydrogen bond with halide directly, the N−H mode of the Schiff base is upshifted as halide size becomes larger even in a protein environment. However, observation of the X−H stretching vibrations has been extremely difficult for rhodopsins because the strong absorption of water masks the signal.

In 1998, we reported accurate K minus BR difference spectra at 77 K for the entire X−H (X−D in D_2O) stretching region (4000−1800 cm^{-1}), which was made possible by optimization of the measuring conditions for low-temperature FTIR spectroscopy (*14*). This progress allowed direct detection of the Schiff base N−D stretch and water O−D stretch in D_2O. In fact, we reported the N−D stretches of the Schiff base in BR to be 2173 and 2123 cm^{-1} (*15*), which exhibit a large frequency shift to 2495 and 2468 cm^{-1} in BR_K. We also observed very low frequency O−D stretch of the bridging water at 2171 cm^{-1} (*16*, *17*), which is considerably weakened in BR_K. Strong hydrogen-bonding interaction of the Schiff base and the bridging water in BR is consistent with the structure (*6*), and transient weakening of these interactions must lead to proton transfer reaction in BR. Recently, the measurements were also extended to the late intermediates of BR (*18*) and other rhodopsins (*19*, *20*). In the case of HR, our FTIR study revealed the absence of strongly hydrogen-bonded water molecules in *s*HR and *p*HR (*21*), which is consistent with the location of the "bridge" water not in the ideal position.

In this article, we studied hydrogen-bonding alterations of the Schiff base and internal water molecules in *p*HR by means of low-temperature FTIR spectroscopy. We trapped pHR_K, pHR_{L1}, and pHR_{L2} at 77, 170, and 250 K, respectively, and difference FTIR spectra were obtained for *p*HR containing Cl^-, Br^-, and I^-. N−D stretch of the Schiff base was assigned by use of [ζ-^{15}N]Lys-labeled *p*HR, while O−D stretches of water were assigned by comparing spectra in D_2O and $D_2{}^{18}O$. We found that the hydrogen bonds of the Schiff base and water molecules are weak in the unphotolyzed state, whereas they are strengthened upon retinal photoisomerization. Halide dependence of the stretching vibrations enabled us to conclude that the Schiff base forms a direct hydrogen bond with Cl^- only in pHR_K. The hydrogen bond of the Schiff base is further strengthened in pHR_{L1}, whereas halide dependence revealed that the acceptor is not Cl^-, but presumably a water molecule. On the basis of the present results, we propose a model of the chloride ion pump. According to the model, removal of hydrogen bonds of Cl^- with the Schiff base and water(s) makes the environment around Cl^- less polar in pHR_{L1}, which drives the translocation of Cl^- from its binding site to the cytoplasmic domain.

MATERIALS AND METHODS

*p*HR was expressed in *Escherichia coli* (*22*), and the purified protein was reconstituted into phosphatidylcholine liposomes (*23*). [ζ-^{15}N]Lys-labeled *p*HR was prepared as was done for [ζ-^{15}N]Lys-labeled *pharaonis* phoborhodopsin (*24*). The sample films were prepared by drying *p*HR in 2 mM phosphate buffer (pH 7.0) containing 5 mM NaCl, NaBr, or NaI. The films were hydrated by 1 μL of D_2O or $D_2{}^{18}O$, and mounted in an Oxford DN-1704 cryostat. FTIR spectra were recorded by a Bio-Rad FTS-40 spectrometer as described previously (*14*−*21*).

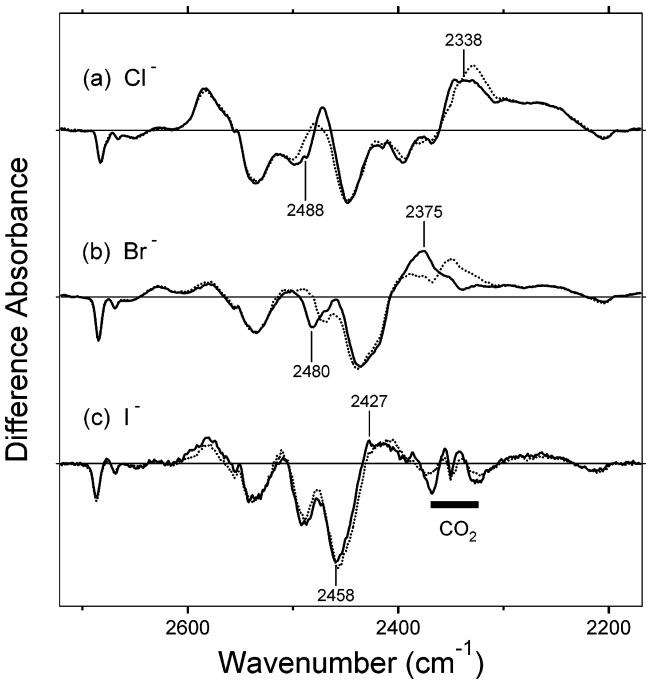

FIGURE 2: The pHR$_K$ minus pHR difference infrared spectra of unlabeled (solid traces) and [ζ-^{15}N]Lys-labeled (dotted traces) pHR in the 2720−2170 cm^{-1} region. The sample containing Cl$^-$ (a), Br$^-$ (b), or I$^-$ (c) was hydrated with D_2O, and spectra were measured at 77 K (130 K for I$^-$). One division of the y axis corresponds to 0.0013 absorbance unit. The spectra in (a) are shown without changing the amplitude, while those in (b) and (c) are multiplied by the factors 0.7 and 2.5, respectively, for the sake of comparison. Spectral artifacts due to fluctuation in CO_2 concentration could not be canceled only in Figure 2c (2380−2310 cm^{-1}) because of the small amplitude of the signal.

The pHR$_K$ minus pHR spectra were obtained by illumination with a 500 nm light (through an interference filter) for 2 min at 77 K as described elsewhere (*21*). The accumulation of the photoproduct of the 13-cis form at 77 K was observed in I$^-$ to a greater extent than in Cl$^-$ and Br$^-$. Since amplitude of this photoproduct was reduced at 130 K, we measured the pHR$_K$ minus pHR spectra in I$^-$ at 130 K. The difference IR spectra in Cl$^-$ in the 1800−800 cm^{-1} region are similar to those reported previously (*25*). The pHR$_{L1}$ minus pHR spectra were obtained by illumination with a >600 nm light at 170 K. Difference FTIR spectra at 230−250 K were obtained by subtracting the spectra taken before illumination from the spectra taken during illumination as described previously (*26*). Five to seven independent measurements with 128 interferograms were averaged.

RESULTS

Hydrogen-Bonding Alterations of the Schiff Base and Water Molecules in the K Photointermediate of pHR. The pHR$_K$ minus pHR spectra were first measured for various halides. All spectra showed the appearance of a positive band at 1198 cm^{-1}, which is characteristic of the formation of the 13-cis form (data not shown). This indicates the formation of the K-like products for all halides as suggested for the Cl$^-$ form previously (*25*). Figure 2 compares the X−D stretching frequency region of the pHR$_K$ minus pHR spectra between unlabeled (solid traces) and [ζ-^{15}N]Lys-labeled (dotted traces) pHR containing various halides. In the presence of Cl$^-$ (Figure 2a), both spectra coincide well except at ∼2480 and ∼2330 cm^{-1}, indicating that the negative 2488 cm^{-1} and positive 2338 cm^{-1} bands originate from the N−D stretching vibrations of the Schiff base in pHR and pHR$_K$, respectively. It is noted that the isotope-induced downshift of the negative band at 2488 cm^{-1} is not clearly observed because of the presence of some positive bands in this region. However, if we subtract the ^{15}N labeled spectrum from the unlabeled one, the isotope effect of the negative 2488 cm^{-1} for pHR is clearly seen (data not shown). The high frequency of the N−D stretch (2488 cm^{-1}) is in clear contrast to those of BR (2173 and 2123 cm^{-1}) (*15*) and ppR (2140 and 2091 cm^{-1}) (*24*), which pump protons. In BR and ppR, the hydrogen-bonding acceptor is a water bridging the Schiff base and the counterion, Asp85 and Asp75, respectively, and photoisomerization weakens the hydrogen bond as shown by the upshifts of the N−D stretch to 2495 and 2468 cm^{-1} in BR (*15*) and to 2474 cm^{-1} in ppR (*24*). A weakened hydrogen bond is the consequence of the motion of the Schiff base, which is consistent with the X-ray crystallographic structures of BR$_K$ (*27*−*29*) and ppR$_K$ (*30*), and theoretical calculations for BR$_K$ (*31*). Interestingly, photoisomerization in pHR yields a stronger hydrogen bond of the Schiff base, as follows from the N−D stretch downshift to 2338 cm^{-1} in pHR$_K$.

In the presence of Br$^-$ (Figure 2b), only the bands at 2480 (−)/2375 (+) cm^{-1} exhibit an isotope shift of [ζ-^{15}N]Lys. Amplitudes of the spectral changes were 2−3 times smaller in the case of I$^-$ (Figure 2c), so that spectral artifacts due to fluctuations of CO_2 concentration could not be entirely canceled in the 2380−2310 cm^{-1} region. However, a clear isotope shift was observed for the positive 2427 cm^{-1} band. Although the isotope shift was small, we assigned the negative band at 2458 cm^{-1} as the N−D stretch of the Schiff base in pHR. An isotope shift of the 2458 cm^{-1} band is observed in the pHR$_{L1}$ minus pHR spectra more clearly (see below). Thus, we assigned the Schiff base N−D stretches in pHR as 2488 (in Cl$^-$), 2480 (Br$^-$), and 2458 (I$^-$) cm^{-1}, and those in pHR$_K$ as 2338 (Cl$^-$), 2375 (Br$^-$), and 2427 (I$^-$) cm^{-1}.

It should be noted that the N−H stretching frequencies of the all-trans retinal Schiff base in solution are located at 2600, 2735, and 2957 cm^{-1} in the presence of Cl$^-$, Br$^-$, and I$^-$, respectively (*13*). Corresponding N−D stretching frequencies are located at 1900−2150 cm^{-1}. In solution, where the Schiff base N−H group forms a hydrogen bond with halides directly, the stretching frequency of the Schiff base is upshifted as halide size becomes larger. Halide dependence of the Schiff base N−D stretch for pHR$_K$ is similar to that in solution, whereas it has an opposite direction for the unphotolyzed state of pHR. These results suggest that the Schiff base does not form a direct hydrogen bond with halide ion in pHR, but photoisomerization leads to a direct hydrogen bond between the Schiff base and halide ion in pHR$_K$. This view for pHR is consistent with the structure of sHR, where the N−H group does not point toward chloride (Figure 1b). A water molecule (water22 in sHR) can be a hydrogen-bonding acceptor of the Schiff base, as the hydrogen bond is weak in pHR.

Figure 3 shows O−D stretching vibrations of water in the pHR$_K$ minus pHR spectra, where isotope shifts were observed for many bands in contrast to Figure 2. In the Cl$^-$ bound form, four negative and positive bands exhibit ^{18}O water-

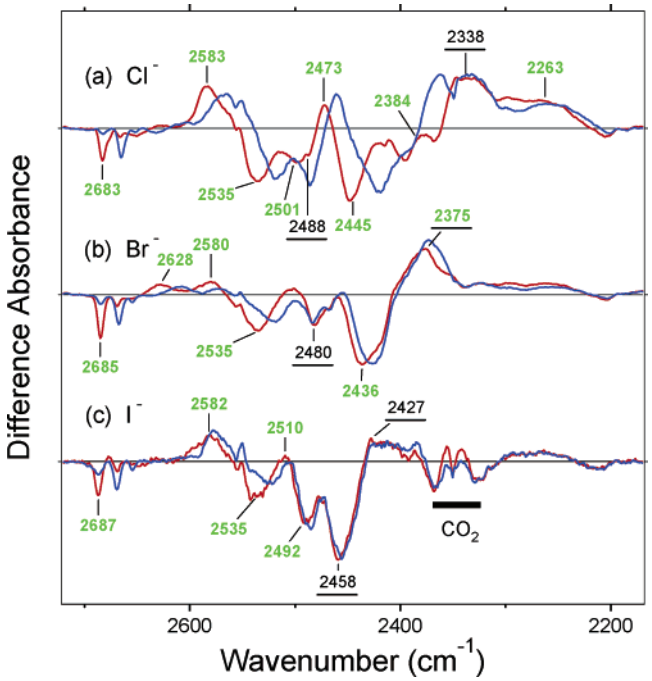

FIGURE 3: The *p*HR$_K$ minus *p*HR difference infrared spectra of the Cl^- (a), Br^- (b), or I^- (c) bound form in the 2720−2170 cm^{-1} region. The sample was hydrated with D_2O (red curves) or $D_2{}^{18}O$ (blue curves), and spectra were measured at 77 K (130 K for I^-). Green-labeled and underlined frequencies correspond to those identified as stretching vibrations of water O−D and the Schiff base N−D, respectively. One division of the *y* axis corresponds to 0.0013 absorbance unit. Scaling and CO_2 artifacts were the same as in Figure 2.

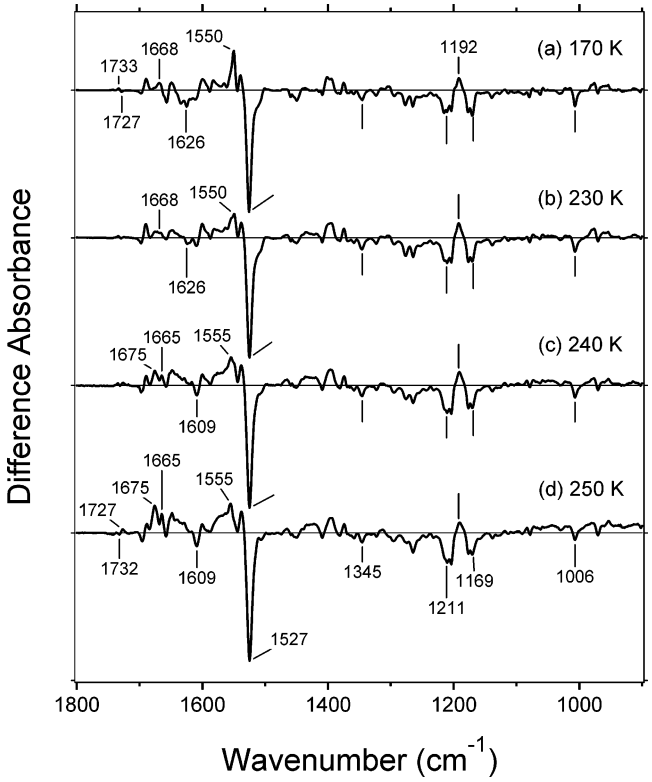

FIGURE 4: The difference infrared spectra of *p*HR in the 1800−900 cm^{-1} region. The sample containing Cl^- was hydrated with D_2O, and spectra were measured at 170 K (a), 230 K (b), 240 K (c), and 250 K (d). One division of the *y* axis corresponds to 0.025 absorbance unit.

induced isotope shifts at 2683, 2535, 2501, and 2445 cm^{-1}, and at 2583, 2473, 2384, and 2263 cm^{-1}, respectively (Figure 3a). Three negative and positive bands were observed at 2685, 2535, and 2436 cm^{-1}, and at 2628, 2580, and 2375 cm^{-1}, respectively, in the Br^- bound form (Figure 3b). While there were three negative bands at 2687, 2535, and 2492 cm^{-1} in the I^- bound form, only two positive bands were observed at 2582 and 2510 cm^{-1} (Figure 3c). These facts imply that at least two water molecules are present near the chromophore, and they change their hydrogen bonds upon retinal photoisomerization.

Among the four water bands of *p*HR(Cl^-), the O−D stretch at 2683 cm^{-1} corresponds to a water with no hydrogen bonds, while those at 2535, 2501, and 2445 cm^{-1} correspond to waters under hydrogen-bonding conditions (Figure 3a). No hydrogen-bonded O−D stretch of water at 2683 cm^{-1} implies the other O−D group of this water molecule being hydrogen bonded. The frequency of the 2683 cm^{-1} band was slightly influenced by different halides, suggesting that the water is present in the halide-binding domain. The frequency of the 2535 cm^{-1} band was insensitive to different halides. Therefore, the hydrogen-bonding acceptor of this water molecule is not a halide. In contrast, the frequencies of the 2501 and 2445 cm^{-1} bands significantly vary in other halides, implying that these water molecules hydrate a halide. It should be however noted that the frequencies are much higher than that for BR (2171 cm^{-1}), indicating that hydrogen-bonding interaction of these waters with halide is much weaker than that of the water with Asp85 in BR.

Upon formation of *p*HR$_K$, the water band at about 2583 cm^{-1} seems to be insensitive to different halides. This band may thereby correspond to the O−D stretch of *p*HR at 2535 cm^{-1}. Other water bands of *p*HR$_K$ were highly dependent on halides. The water O−D stretch at 2263 cm^{-1} (Figure 3a) is particularly interesting. The low frequency observed in the Cl^- form implies that the retinal isomerization induces formation of a strong hydrogen bond of water. In the Br^- form, the corresponding water band is probably at 2375 cm^{-1} (Figure 3b), which appears in the same frequency region as the N−D stretch of the Schiff base (Figure 2b). No such band was observed in the I^- form (Figure 3c). Strong halide dependence of the water band suggests that the hydrogen-bonding acceptor is the halide. Rotational motion of water presumably leads to a strong hydrogen bond with Cl^- or Br^-, where the water O−D group points toward the halide. On the other hand, larger size may prohibit strong interaction of the water with I^-.

Hydrogen-Bonding Alterations of the Schiff Base and Water Molecules in the L_1 Photointermediate of pHR. The decay of the K intermediate accompanies formation of the L intermediate. UV−visible spectroscopy showed formation of the L intermediate at 170 and 250 K. Figure 4 shows the *p*HR$_L$ minus *p*HR spectra (D_2O) in the presence of Cl^-. Identical fingerprint vibrations at 1211 (−), 1192 (+), and 1169 (−) cm^{-1} between 170 and 250 K indicate formation of the L intermediate in *p*HR. Nevertheless, we found that the amide-I and -II regions of the FTIR spectra are different among temperatures. In fact, a positive peak at 1550 cm^{-1} (Figure 4a) is shifted to 1555 cm^{-1} as temperature is increased (Figure 4c,d). Similar visible absorption implies that the spectral change originates from amide-II vibration of the peptide backbone. Similarly, a clear spectral difference

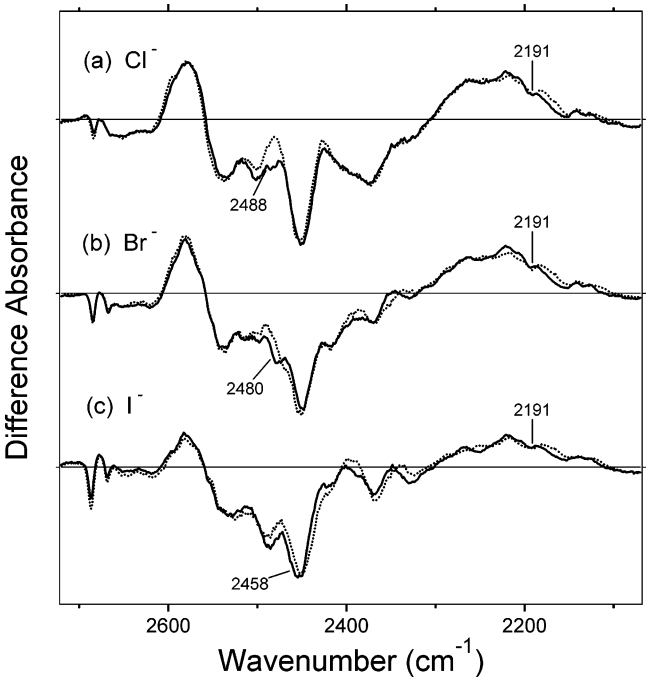

FIGURE 5: The pHR$_{L1}$ minus pHR difference infrared spectra of unlabeled (solid traces) and [ζ-^{15}N]Lys-labeled (dotted traces) pHR in the 2720−2070 cm^{-1} region. The sample containing Cl$^-$ (a), Br$^-$ (b), or I$^-$ (c) was hydrated with D_2O, and spectra were measured at 170 K. One division of the y axis corresponds to 0.002 absorbance unit. The spectra in (a) are shown without changing the amplitude, while those in (b) and (c) are multiplied by the factors 0.78 and 2.0, respectively, for the sake of comparison.

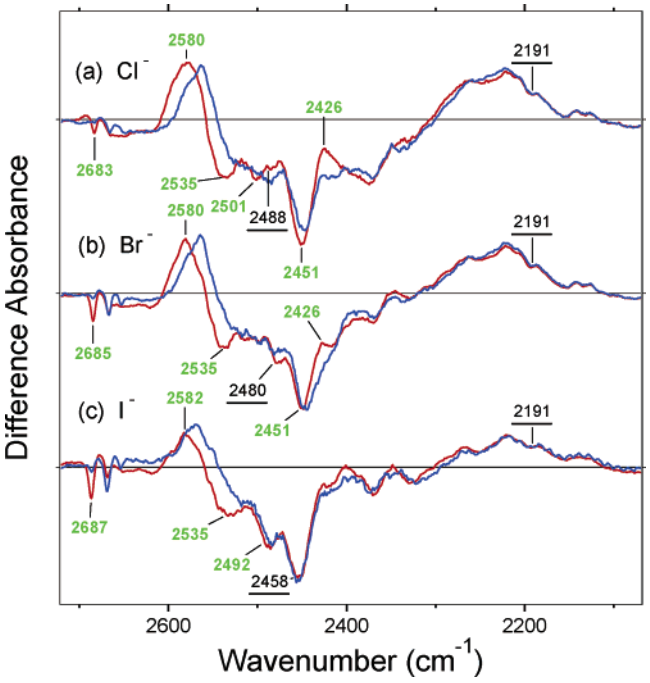

FIGURE 6: The pHR$_{L1}$ minus pHR difference infrared spectra of the Cl$^-$ (a), Br$^-$ (b), or I$^-$ (c) bound form in the 2720−2070 cm^{-1} region. The sample was hydrated with D_2O (red curves) or $D_2{}^{18}O$ (blue curves), and spectra were measured at 170 K. Green-labeled and underlined frequencies correspond to those identified as stretching vibrations of water O−D and the Schiff base N−D, respectively. One division of the y axis corresponds to 0.002 absorbance unit. Scaling was the same as in Figure 5.

was observed in the amide-I region. The negative 1626 cm^{-1} band at 170 K is diminished at 250 K, where the strongest negative peak is located at 1609 cm^{-1}. The positive 1668 cm^{-1} band at 170 K is shifted to 1665 cm^{-1} at 250 K. In addition, a new peak appears at 1665 cm^{-1} (Figure 4c,d). Spectral change of the carboxylic C=O stretch region is also different: 1733 (+)/1727 (−) cm^{-1} and 1732 (−)/1727 (+) cm^{-1} at 170 and 250 K, respectively. These results indicate the presence of the two L intermediate states for pHR. Two such temperature-dependent forms of the L intermediate were also observed for sHR (*26*). Accordingly, we define the photointermediates at 170 and 250 K as L_1 and L_2, respectively.

Figure 5 compares the X−D stretching frequency region of the pHR$_{L1}$ minus pHR spectra of unlabeled (solid traces) and [ζ-^{15}N]Lys-labeled (dotted traces) pHR containing various halides. In the presence of Cl$^-$ (Figure 5a), no clear isotope effect was observed for the negative side except for the 2500−2480 cm^{-1} region, where the negative band shows reduced the intensity in the ^{15}N labeled spectrum. Figure 2a showed the presence of the N−D stretch of pHR (Cl$^-$) at 2488 cm^{-1}, which strongly suggests the presence of the same negative band in Figure 5a. No clear isotope-induced downshift for the 2488 cm^{-1} band may originate from strong O−D absorption of hydrated D_2O in the same frequency region, by which the baseline is considerably fluctuated. In contrast, the spectra in Figure 5b and Figure 5c exhibit isotope shifts for the negative features at 2480 and 2458 cm^{-1}, respectively. Thus, the N−D stretch of the Schiff base in pHR was assigned as 2488 (Cl$^-$), 2480 (Br$^-$), and 2458 (I$^-$) cm^{-1} from Figure 5, as is the case in the pHR$_K$ minus pHR spectra. In contrast, a single positive band at 2191 cm^{-1} exhibits an isotope shift of [ζ-^{15}N]Lys in all cases (Figure 5a−c). The spectra possess broad positive absorption in the 2300−2100 cm^{-1} region, but isotope shifts of [ζ-^{15}N]Lys were only observed at 2200−2180 cm^{-1} (Figure 5). Other bands may originate from amide-A vibrations of peptide backbone.

In this way, we assigned the Schiff base N−D stretch in pHR$_{L1}$ as 2191 cm^{-1}. It should be noted that the frequency of the N−D stretch of the Schiff base is much lower in pHR$_{L1}$ than in pHR and pHR$_K$ for all halides, indicating that the hydrogen bond of the Schiff base is strong in pHR$_{L1}$. On the other hand, lack of halide dependence strongly suggests that the Schiff base does not form a hydrogen bond with halide in pHR$_{L1}$.

Figure 6 shows O−D stretching vibrations of water in the pHR$_{L1}$ minus pHR spectra. In the Cl$^-$ bound form, four negative bands exhibit an isotope shift of ^{18}O water (Figure 6a), which were also observed in the pHR$_K$ minus pHR spectrum (Figure 3a). In contrast, only one positive peak was observed at 2580 cm^{-1}. In addition, there seems to be a positive band at 2426 cm^{-1}, though it does not appear to the positive side. Similarly, three negative bands of water were observed in Br$^-$ (Figure 6b) and I$^-$ (Figure 6c), which also appeared in the pHR$_K$ minus pHR spectra. The negative bands at 2436 cm^{-1} in Figure 3b and at 2451 cm^{-1} in Figure 6b presumably have the same origin for pHR(Br$^-$). The presence of the same negative water bands between pHR$_K$ minus pHR (77 K) and pHR$_{L1}$ minus pHR (170 K) spectra implies that only water molecules located near the retinal change their hydrogen bonds in pHR$_{L1}$. In other words, there are no additional water molecules altering their hydrogen bonds in pHR$_{L1}$ as compared to pHR$_K$.

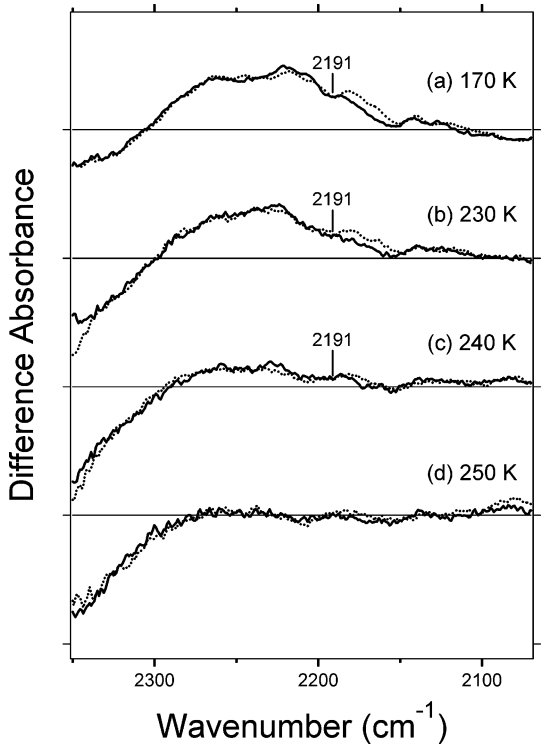

FIGURE 7: Infrared difference spectra of unlabeled (solid traces) and [ζ-^{15}N]Lys-labeled (dotted traces) *p*HR in the 2350−2070 cm^{-1} region. The sample containing Cl^- was hydrated with D_2O, and spectra were measured at 170 K (a), 230 K (b), 240 K (c), and 250 K (d). One division of the *y* axis corresponds to 0.001 absorbance unit. All spectra are shown without changing the amplitudes.

It is noted that positive bands of water in Figure 3 (for pHR_K) were highly halide-dependent, but not in Figure 6 (for pHR_{L1}). In fact, spectra are similar among three halides in Figure 6, while being different in Figure 3. A positive band of water was observed at about 2580 cm^{-1} for all halides. Another positive band at 2426 cm^{-1} is common between $pHR_{L1}(Cl^-)$ and $pHR_{L1}(Br^-)$. Although it is absent in $pHR_{L1}(I^-)$, identical frequency between Cl^- and Br^- strongly suggests that internal water molecules do not hydrate halide in pHR_{L1}, being in clear contrast to *p*HR and pHR_K. The environment surrounding halide seems to become less polar in pHR_{L1}, which could provide driving force of the translocation of halide.

Hydrogen-Bonding Alterations of the Schiff Base in the L_2 Photointermediate of pHR. Figure 7 shows the difference FTIR spectra between unlabeled (solid traces) and [ζ-^{15}N]-Lys-labeled (dotted traces) $pHR(Cl^-)$ in the 2350−2070 cm^{-1} region. The spectra at 170 and 250 K are characteristic pHR_{L1} minus *p*HR and pHR_{L2} minus *p*HR spectra, respectively. It should be noted that the measurements at the different temperatures produced identical spectra with the same amplitudes for the fingerprint (1300−1100 cm^{-1}) and HOOP (1000−900 cm^{-1}) vibrations of the retinal chromophore, whereas those in the amide-I region were different (Figure 4). Figure 7 shows that strong positive absorption in the 2300−2100 cm^{-1} region at 170 K is reduced at higher temperatures. At 250 K, where only pHR_{L2} is formed, positive absorption has completely disappeared, and there are no isotope effects of [ζ-^{15}N]Lys at <2350 cm^{-1} (Figure 7d). These results indicate that the N−D stretch of the Schiff base appears at >2350 cm^{-1} in pHR_{L2}.

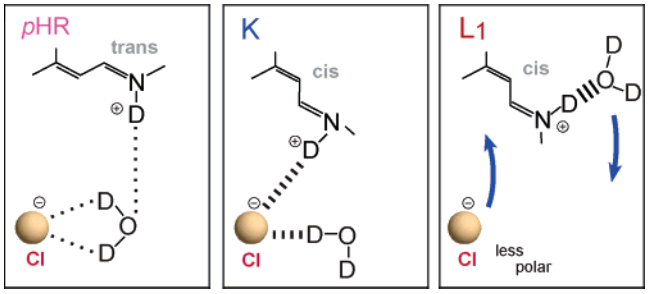

FIGURE 8: Schematic drawing of the hydrogen-bonding interaction of the Schiff base and water molecule with chloride based on present FTIR results. Blue arrows indicate the hypothetical motion of Cl^- and water in the conversion from pHR_{L1} to pHR_{L2}.

Because of baseline distortions at 250 K, we could not observe the accurate difference absorption spectra at >2350 cm^{-1}, so that the frequencies of the N−D stretch of the Schiff base and O−D stretches of water molecules were not obtained in the present study. Therefore, the N−D stretch of the Schiff base in $pHR(Cl^-)$ appears at 2488 cm^{-1} in *p*HR, 2338 cm^{-1} in pHR_K, 2191 cm^{-1} in pHR_{L1}, and >2350 cm^{-1} in pHR_{L2}.

DISCUSSION

Hydrogen-bonding strengths of the Schiff base in HR and its intermediates have been discussed only on the basis of the C═N stretching vibrations among various halides (*11*, *12*). However, the C═N stretch is a skeletal vibration of the retinal chromophore, and even when the C═NH and C═ND frequency difference explains the hydrogen-bonding strength of the Schiff base well, halide dependence on the C═N stretch does not necessarily reflect hydrogen-bonding interaction of the Schiff base with halides. A more direct probe of the hydrogen-bonding strength is the N−H (N−D) stretch of the Schiff base. The present low-temperature FTIR spectroscopic study successfully assigned the vibrational frequencies of the N−D stretch of the Schiff base and O−D stretches of internal water molecules in *p*HR, pHR_K, and pHR_{L1}. The N−D stretch of the Schiff base in pHR_{L2} was also found to be at >2350 cm^{-1}. In addition, variations of the spectra in three halides (Cl^-, Br^-, and I^-) could provide direct information on how halide interacts with the Schiff base and water molecules. In solution, the stretching vibration of the protonated Schiff base of all-trans retinal appears at higher frequency if halide size is increased (*13*). A similar tendency was observed only for pHR_K. Halide dependence for *p*HR was opposite to that in solution, whereas no halide dependence was observed for pHR_{L1}. These observations enabled us to propose a model for the early stages of chloride ion transport in *p*HR (Figure 8).

Hydrogen Bonds in the Schiff Base Region of pHR. In the unphotolyzed state of *p*HR, the N−D stretch of the Schiff base is at 2488 cm^{-1}, sign of a weak hydrogen-bonding. We assigned the N−D stretches of BR and *p*pR as 2173 and 2123 cm^{-1} (*15*), and 2140 and 2091 cm^{-1} (*24*), respectively. N−D stretches of the Schiff base in *Neurospora* rhodopsin and bovine rhodopsin are likely to be at 2173 and 2123 cm^{-1} (*20*) and at about 2000 cm^{-1} (*19*), respectively, though not assigned by [ζ-^{15}N]Lys labeling. It is in prominent contrast that *p*HR possesses weakly hydrogen-bonded Schiff base. A weak hydrogen bond of the Schiff base was reported by

the analysis of the difference between C=NH and C=ND stretches by the earlier resonance Raman spectroscopy of *s*HR (*9*).

In *s*HR, it is likely that the Schiff base does not form a hydrogen bond with halide directly (Figure 1b). Nevertheless, the Schiff base vibrations can be influenced by size changes of the halide ion, because of the close distance between chloride and the Schiff base nitrogen (3.7 Å). We assume a similar binding site of chloride in *p*HR. Since the halide dependence of the N−D stretching frequency in *p*HR was opposite to that in solution, the Schiff base does not form a direct hydrogen bond with chloride. On the other hand, opposite halide dependence suggests that the chloride binding site is close to the Schiff base as in *s*HR. The presence of halide-dependent water O−D stretching (2501 and 2445 cm^{-1} for Cl^-; Figure 3) implies that this water hydrates with chloride. Thus, the structure of this region in *s*HR (Figure 1b) explains the present observation for *p*HR well. A recent mutation study also supported a similar environment of the Schiff base between *p*HR and *s*HR (*32*). It should be noted that the $N-O_{water}$ and $O_{water}-Cl$ distances are 3.3 and 3.1 Å, respectively, and the $N-O_{water}-Cl$ angle is 70.9° in *s*HR (Figure 1b), suggesting that water22 cannot form a full hydrogen bond both with the Schiff base and with chloride. A weak hydrogen bond of the Schiff base implies that the interaction between chloride and water is stronger than that between the Schiff base and water in *p*HR. Previous neutron diffraction studies of aqueous hydrochloric acid solutions reported that water molecules around a chloride ion take the configuration to orient the vector which bisects the D−O−D angle on a straight line joining an oxygen atom and chloride (*33*, *34*). In other words, each deuterium atom is not located on a straight line between the oxygen and chloride, suggesting that the hydrogen bond of the O−D groups of water22 is not strong (Figure 1). Thus, the hydrogen-bonding structure of the Schiff base region in *p*HR may be as shown in Figure 8.

Hydrogen Bonds in the Schiff Base Region of pHR_K. Retinal photoisomerization strengthens the hydrogen bond of the Schiff base. The identical halide dependence between *p*HR_K and solution strongly suggests that the Schiff base forms a direct hydrogen bond with chloride (Figure 8). If Cl^- binds to the same site in *p*HR as in *s*HR (Figure 1a), the present observation may indicate direction of the motion of the Schiff base. At 77 K, Cl^- is not likely to move, suggesting that the N−H (N−D in this case) group rotates clockwise in Figure 1a. This is the direction opposite to that in BR, where the counterclockwise rotation reorients the N−H group toward helix G (*27*, *28*, *30*).

It is of interest that formation of *p*HR_K, the red-shifted intermediate, accompanies a stronger hydrogen bond of the Schiff base for *p*HR. This may be apparently controversial, because a stronger hydrogen bond of the Schiff base generally yields a spectral blue-shift. In fact, formation of the K intermediates of BR and *p*pR accompanies a significantly weakened hydrogen bond of the Schiff base (*15*, 24), which is consistent with the above view. Thus, the present result for *p*HR provides the complexity of color tuning mechanism in rhodopsins. Another exceptional case is seen for bovine rhodopsin. Bathorhodopsin is a red-shifted intermediate of rhodopsin, whereas its hydrogen-bonding strength of the Schiff base is almost identical to that of rhodopsin (*19*). In the case of *p*HR and rhodopsin, other factors such as chromophore distortion may be dominant for color tuning mechanism of the primary intermediates.

Hydrogen Bonds in the Schiff Base Region of pHR_{L1} and pHR_{L2}. One of the most important findings in the present study is the absence of the halide dependence of the N−D stretch of the Schiff base in *p*HR_{L1}, although the hydrogen bond in *p*HR_{L1} is much stronger than in *p*HR, *p*HR_K, and *p*HR_{L2}. This observation strongly suggests that Cl^- is not the hydrogen-bonding acceptor of the Schiff base in *p*HR_{L1}. Stronger hydrogen bond in *p*HR_L is consistent with the previous resonance Raman study of *s*HR (*10*). On the other hand, the present conclusion is in contrast to Gerscher et al., which argued that the Schiff base directly interacts with chloride in *p*HR_L as inferred from the halide dependence of the C=N stretch (*11*). It must be however noted that the C=N stretch itself is not a measure of the hydrogen-bonding strength of the Schiff base, and the frequency can be affected by various factors.

What is the hydrogen-bonding acceptor of the Schiff base in *p*HR_{L1}? Although the present study does not provide a direct answer, an implication was obtained from Figure 6. Unlike for *p*HR_K (Figure 3), no halide dependence was observed for the O−D stretches of water in *p*HR_{L1}. This fact suggests that hydrogen bonds between water and halide are diminished in *p*HR_{L1}. Thus, we propose the structural model for *p*HR_{L1} as shown in Figure 8. The retinal chromophore is in a relaxed 13-cis form, where the N−D group of the Schiff base points toward the cytoplasmic side (upward in Figure 8). The hydrogen-bonding acceptor is a water molecule. In this model, the position of Cl^- is not altered throughout *p*HR, *p*HR_K, and *p*HR_{L1}, whereas hydrogen-bonding interaction with Cl^- differs significantly. The structural model in Figure 8 also suggests the mechanism of the initial translocation of Cl^- during the pump cycle. Because of the lack of hydrogen bonds with the Schiff base and water, the environment around Cl^- becomes less polar in *p*HR_{L1}. This presumably drives the movement of Cl^- in the *p*HR_{L1} to *p*HR_{L2} transition. Electrostatic repulsion with Asp252 may also contribute to it. It is however noted that the present study did not determine the position of Cl^- in *p*HR_{L1}. Our model for chloride transport in Figure 8 depends entirely on Cl^- being on the extracellular side of the Schiff base in *p*HR_{L1}. It is probably most straightforward from the results, but it may be possible that the movement of Cl^- takes place upon formation of *p*HR_{L1}. Thus, the question of when Cl^- moves is once again open by the present study. Further experimental efforts such as halide dependence on protein bands will answer the question in the future.

ACKNOWLEDGMENT

We thank Dr. Yuji Furutani for valuable discussion.

REFERENCES

1. Haupts, U., Tittor, J., and Oesterhelt, D. (1999) Closing in on bacteriorhodopsin: progress in understanding the molecules, *Annu. Rev. Biophys. Biomol. Struct. 28*, 367−399.
2. Lanyi, J. K. (2004) Bacteriorhodopsin, *Annu. Rev. Physiol. 66*, 665−688.
3. Váró, G. (2000) Analogies between halorhodopsin and bacteriorhodopsin, *Biochim. Biophys. Acta 1460*, 220−229.
4. Essen, L.-O. (2002) Halorhodopsin: light-driven ion pumping made simple?, *Curr. Opin. Struct. Biol. 12*, 516−522.

5. Kolbe, M., Besir, H., Essen, L.-O., and Oesterhelt, D. (2000) Structure of the light-driven chloride pump halorhodopsin at 1.8 Å resolution, *Science 288*, 1390−1396.
6. Luecke, H., Schobert, B., Richter, H.-T., Cartailler, J. P., and Lanyi, J. K. (1999) Structure of bacteriorhodopsin at 1.55 Å resolution, *J. Mol. Biol. 291*, 899−911.
7. Aton, B., Doukas, A. G., Callender, R. H., Becher, B., and Ebrey, T. G. (1977) Resonance Raman studies of the purple membrane, *Biochemistry 16*, 2995−2999.
8. Baasov, T., Friedman, N., and Sheves, M. (1987) Factors affecting the C=N stretching in protonated retinal Schiff base: a model study for bacteriorhodopsin and visual pigments, *Biochemistry 26*, 3210−3217.
9. Smith, S. O., Marvin, M. J., Bogomolni, R. A., and Mathies, R. A. (1984) Structure of the retinal chromophore in the hR578 form of the halorhodopsin, *J. Biol. Chem. 259*, 12326−12329.
10. Fodor, S. P. A., Bogomolni, R. A., and Mathies, R. A. (1987) Structure of the retinal chromophore in the hR_L intermedeiate of halorhodopsin from resonance spectroscopy, *Biochemistry 26*, 6775−6778.
11. Gerscher, S., Mylrajan, M., Hildebrandt, P., Baron, M.-H., Müller, R., and Engelhard, M. (1997) Chromophore-anion interactions in halorhodopsin form *Natronobacterium pharaonis* probed by time-resolved resonance Raman spectroscopy, *Biochemistry 36*, 11012−11020.
12. Walter, T. J., and Braiman, M. S. (1994) Anion-protein interactions during halorhodopsin pumping: halide binding at the protonated Schiff base, *Biochemistry 33*, 1724−1733.
13. Lussier, L. S., Sandorfy, C., Le-Thanh, H., and Vocelle, D. (1987) Effect of acids on the infrared spectra of the Schiff base of *trans*-retinal, *J. Phys. Chem. 91*, 2282−2287.
14. Kandori, H., Kinoshita, N., Shichida, Y., and Maeda, A. (1998) Protein structural changes in bacteriorhodopsin upon photoisomerization as revealed by polarized FTIR spectroscopy, *J. Phys. Chem., B 102*, 7899−7905.
15. Kandori, H., Belenky, M., and Herzfeld, J. (2002) Vibrational frequency and dipolar orientation of the protonated Schiff base in bacteriorhodopsin before and after photoisomerization, *Biochemistry 41*, 6026−6031.
16. Kandori, H., and Shichida, Y. (2000) Direct observation of the bridged water stretching vibrations inside a protein, *J. Am. Chem. Soc. 122*, 11745−11746.
17. Shibata, M., Tanimoto, T., and Kandori, H. (2003) Water molecules in the Schiff base region of bacteriorhodopsin, *J. Am. Chem. Soc. 125*, 13312−13313.
18. Tanimoto, T., Furutani, Y., and Kandori, H. (2003) Structural changes of water in the Schiff base region of bacteriorhodopsin: proposal of a hydration switch model, *Biochemistry 42*, 2300−2306.
19. Furutani, Y., Shichida, Y., and Kandori, H. (2003) Structural changes of water molecules during the photoactivation processes in bovine rhodopsin, *Biochemistry 42*, 9619−9625.
20. Furutani, Y., Bezerra, A. G., Jr., Waschuk, S., Sumii, M., Brown, L. S., and Kandori, H. (2004) FTIR spectroscopy of the K photointermediate of *Neurospore* rhodopsin: structural changes of the retinal, protein, and water molecules after photoisomerization, *Biochemistry 43*, 9636−9646.
21. Shibata, M., Muneda, N., Ihara, K., Sasaki, T., Demura, M., and Kandori, H. (2004) Internal water molecules of light-driven chloride pump proteins, *Chem. Phys. Lett. 392*, 330−333.
22. Sato, M., Kanamori, T., Kamo, N., Demura, M., and Nitta, K. (2002) Stopped-flow analysis on anion binding to blue-form halorhodopsin from *Natronobacterium pharaonis*: comparison with the anion-uptake process during the photocycle, *Biochemistry 41*, 2452−2458.
23. Kandori, H., Shimono, K., Sudo, Y., Iwamoto, M., Shichida, Y., and Kamo, N. (2001) Structural change of *pharaonis* phoborhodopsin upon photoisomerization of the retinal chromophore: infrared spectral comparison with bacteriorhodopsin, *Biochemistry 40*, 9238−9246.
24. Shimono, K., Furutani, Y., Kamo, N., and Kandori, H. (2003) Vibrational modes of the protonated Schiff base in *pharaonis* phoborhodopsin, *Biochemistry 42*, 7801−7806.
25. Hackmann, C., Guijarro, J., Chizhov, I., Engelhard, M., Rödig, C., and Siebert, F. (2001) Static and time-resolved step-scan Fourier transform infrared investigations of the photoreaction of halorhodopsin from *Natronobacterium pharaonis*: consequences for models of the anion translocation mechanism, *Biophys. J. 81*, 394−406.
26. Chon, Y.-S., Kandori, H., Sasaki, J., Lanyi, J. K., Needleman, R., and Maeda, A. (1999) Existence of two L photointermediates of halorhodopsin from *Halobacterium salinarum*, differing in their protein and water FTIR bands, *Biochemistry 38*, 9449−9455.
27. Edman, K., Nollert, P., Royant, A., Belrhali, H., Pebay-Peyroula, E., Hajdu, J., Neutze, R., and Landau, E. M. (1999) High-resolution X-ray structure of an early intermediate in the bacteriorhodopsin photocycle, *Nature 401*, 822−826.
28. Schobert, B., Cupp-Vickery, J., Hornak, V., Smith, S. O., and Lanyi, J. K. (2002) Crystallographic structure of the K intermediate of bacteriorhodopsin: conservation of free energy after photoisomerization of the retinal, *J. Mol. Biol. 321*, 715−726.
29. Matsui, Y., Sakai, K., Murakami, M., Shiro, Y., Adachi, S., Okumura, H., and Kouyama, T. (2002) Specific damage induced by X-ray radiation and structural changes in the primary photoreaction of bacteriorhodopsin, *J. Mol. Biol. 324*, 469−481.
30. Edman, K., Royant, A., Nollert, P., Maxwell, C. A., Pebay-Peyroula, E., Navarro, J., Neutze, R., and Landau, E. M. (2002) Early structural rearrangements in the photocycle of an integral membrane sensory receptor, *Structure 10*, 473−482.
31. Hayashi, S., Tajkhorshid, E., and Schulten, K. (2002) Structural changes during the formation of early intermediates in the bacteriorhodopsin photocycle, *Biophys. J. 83*, 1281−1297.
32. Sato, M., Kubo, M., Aizawa, T., Kamo, N., Kikukawa, T., Nitta, K., and Demura, M. (2005) Role of putative anion-binding sites in cytoplasmic and extracellular channels of *Natronomonas pharaonis* halorhodopsin, *Biochemistry 44*, 4775−4784.
33. Ohtomo, N., and Arakawa, K. (1980) Neutron diffraction of aqueous ionic solutions. II. aqueous solutions of sodium chloride and potassium chloride, *Bull. Chem. Soc. Jpn. 53*, 1789−1794.
34. Ohtomo, N., Arakawa, K., Takeuchi, M., Yamaguchi, T., and Ohtaki, H. (1981) Neutron diffraction study of aqueous hydrochloric and hydrobromic acid solutions, *Bull. Chem. Soc. Jpn. 54*, 1314−1319.

BI050726D